High accuracy microwave frequency measurement based on single-drive dual-parallel Mach-Zehnder modulator

Zhao, Ying; Pang, Xiaodan; Deng, Lei; Yu, Xianbin; Zheng, Xiaoping; Zhou, Bingkun; Tafur Monroy, Idelfonso

Published in:
Optics Express

Link to article, DOI:
10.1364/OE.19.00B681

Publication date:
2011

Document Version
Publisher's PDF, also known as Version of record

High accuracy microwave frequency measurement based on single-drive dual-parallel Mach-Zehnder modulator

Ying Zhao,[1,2,*] **Xiaodan Pang,**[2] **Lei Deng,**[2,3] **Xianbin Yu,**[2,4] **Xiaoping Zheng,**[1,5] **Bingkun Zhou,**[1] **and Idelfonso Tafur Monroy**[2]

[1]*Department of Electronic Engineering, Tsinghua National Laboratory for Information Science and Technology, Tsinghua University, 100084 Beijing, China*
[2]*DTU Fotonik, Technical University of Denmark, DK-2800, Kgs. Lyngby, Denmark*
[3]*School of Optoelectronics Science & Engineering, HuaZhong University of Science & Technology, Wuhan, China*
[4]*xiyu@fotonik.dtu.dk*
[5]*xpzheng@mail.tsinghua.edu.cn*
** yingzhao840729@gmail.com*

Abstract: A novel approach for broadband microwave frequency measurement by employing a single-drive dual-parallel Mach-Zehnder modulator is proposed and experimentally demonstrated. Based on bias manipulations of the modulator, conventional frequency-to-power mapping technique is developed by performing a two-stage frequency measurement cooperating with digital signal processing. In the experiment, 10GHz measurement range is guaranteed and the average uncertainty of estimated microwave frequency is 5.4MHz, which verifies the measurement accuracy is significantly improved by achieving an unprecedented 10^{-3} relative error. This high accuracy frequency measurement technique is a promising candidate for high-speed electronic warfare and defense applications.

OCIS codes: (060.5625) Radio frequency photonics; (350.4010) Microwaves.

References and links

1. J. Yao, "Microwave Photonics," IEEE J. Lightwave Technol. **27**, 314–335 (2009).
2. G. N. Saddik, R. S. Singh, and E. R. Brown, "Ultra-wideband multifunctional communications/radar system," IEEE Trans. Microw. Theory Tech. **55**, 1431–1437 (2007).
3. I. Frigyes and A. J. Seeds, "Optically generated true-time delay in phased-array antennas," IEEE Trans. Microw. Theory Tech. **43**, 2378–2386 (1995).
4. D. B. Hunter, L. G. Edvell, and M. A. Englund, "Wideband microwave photonic channelised receiver," in *Proceedings of 2005 IEEE Topical Meeting on Microwave Photonics (MWP)*, pp. 249–252.
5. S. T. Winnall, A. C. Lindsay, M. W. Austin, J. Canning, and A. Mitchell, "A microwave channelizer and spectroscope based on an integrated optical Bragg-grating Fabry-Pérot and integrated hybrid fresnel lens system," IEEE Trans. Microw. Theory Tech. **54**, 868–872 (2006).
6. S. Fu, J. Zhou, P. P. Shum, and K. Lee, "Instantaneous microwave frequency measurement using programmable differential group delay (DGD) modules," IEEE Photonics J. **2**, 966–973 (2010).
7. H. Chi, X. Zou, and J. Yao, "An approach to the measurement of microwave frequency based on optical power monitoring," IEEE Photon. Technol. Lett. **20**, 1249–1251 (2008).
8. X. Zou, S. Pan, and J. Yao, "Instantaneous microwave frequency measurement with improved measurement range and resolution based on simultaneous phase modulation and intensity modulation," IEEE J. Lightwave Technol. **27**, 5314–5318 (2009).
9. S. Li, X. Zheng, H. Zhang, and B. Zhou, "Dispersion induced fading frequency shifting technology in Radio-over-Fiber link," in *Proceedings of 2010 IEEE Topical Meeting on Microwave Photonics (MWP)*, pp. 321–322.

#154886 - $15.00 USD Received 19 Sep 2011; revised 4 Nov 2011; accepted 14 Nov 2011; published 5 Dec 2011

1. Introduction

Microwave photonics has driven and facilitated various kinds of applications for its superiority on potential high-speed and parallel microwave signal processing capability [1]. For electronic warfare and defense applications, ultra-fast optical signal processing provides elegant solutions for developing adaptivity and agility of modern electronic countermeasure (ECM) equipments, eg. millimeter-wave phased array radar and spoofing devices [2,3]. Broadband carrier frequency measurement in optical manners can be a key application as well for intercepted signal processing where a high accuracy and large measurement range is required. The primary advantages of photonics-assisted microwave frequency measurement are the broadband and electronic transparency characteristics of lightwave signal. Generally, real-time approaches for microwave frequency measurement are based on spectral or temporal operations of modulated optical carrier. Regarding spectral operation approaches, microwave photonic channelizers realized based on parallel phase-shifted fiber Bragg gratings (FBGs) [4], or based on an integrated optical FBG Fabry-Pérot (F-P) device [5], have been proposed for frequency measurement and spectrum analysis. In the time domain, microwave frequency measurement can be realized by comparing the powers of two microwave signals experiencing different optical links, which is named frequency-to-power mapping technique. Recently, frequency measurement systems based on frequency-to-power mapping have been intensively investigated [6–8]. Complementary filtering implemented by microwave photonic filters [6] are generally adopted while other schemes using multiple laser sources or modulators are developed [7, 8]. The major limitation of previous methods is the comparatively large measurement error (several percent), which prevents them from being used in high accuracy applications.

In this paper, we propose and demonstrate a novel approach for high accuracy frequency measurement based on frequency-to-power mapping technique by using a single-drive dual parallel Mach-Zehnder modulator (SD-DPMZM). The flexibility of the modulator to manipulate lightwave signals is explored with theoretical analysis of the operation principle. By deliberately tuning one of the bias points of the SD-DPMZM, the power fading characteristics of an unknown microwave signal changes, which thereby results in the change of measurement accuracy. The highest accuracy point can be obtained by implementing a two-stage frequency measurement with consecutive procedures. In the experiment, automatic control cooperating with digital signal processing (DSP) is realized to facilitate measurement procedures systematically. The experiment verifies the improved accuracy of this approach by performing a $\sim 10^{-3}$ relative error within a 10GHz measurement range. Detailed measurement performances are investigated as well.

2. Principle

Figure 1 shows the bias arrangement of a DPMZM for frequency measurement purpose. The structure of a DPMZM contains two sub-MZMs, MZM1 and MZM2, lying in parallel on two arms of MZM3. MZM3 is only controlled by the applied bias voltage without RF drive. In the single-drive case, MZM1 is biased at the minimal transmission point (NULL point) and driven by a RF signal with unknown frequency to perform carrier suppressed double sideband (CS-DSB) modulation. MZM2 is remained un-modulated and arbitrarily biased to let the optical carrier propagate through. This asymmetrical arrangement is named single-drive of a DPMZM or CSDSB+Carrier modulation scheme [9]. By employing SD-DPMZM, the phase difference φ_3 between the optical carrier and two first-order sidebands is only determined by the bias point of MZM3 and can be adjusted independently. The purpose of implementing SD-DPMZM is to obtain φ_3-dependent RF power variance after fiber transmission, which is caused by dispersion-induced power fading characteristic of a radio-over-fiber link. As shown in Fig. 1, the absolute power level of the output RF signal can be expressed by

#154886 - $15.00 USD Received 19 Sep 2011; revised 4 Nov 2011; accepted 14 Nov 2011; published 5 Dec 2011

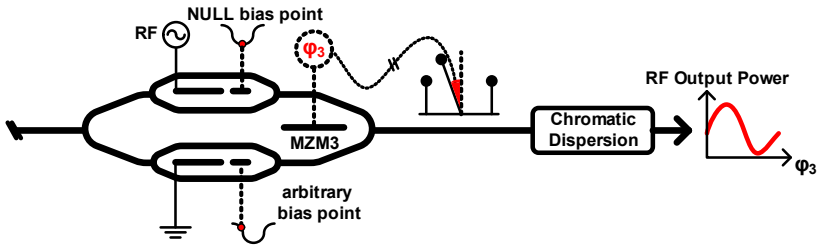

Fig. 1. Bias arrangement of a SD-DPMZM for frequency measurement and the illustrative diagram of RF output power vs φ_3.

$$P_{out}(\varphi_3) \propto \cos^2\left(\frac{\beta_2 \cdot L}{2}\Omega^2 + \varphi_3\right) \tag{1}$$

where β_2 and L are the dispersion coefficient and the length of the fiber link, respectively. Ω is the angular frequency of the unknown RF signal. Since the absolute power level is dependent on various parameters including optical power and detector responsivity etc., it is impossible to correctly calculate the unknown frequency Ω directly from Eq. (1). To avoid using uncertain common-mode parameters and to eliminate undesirable effects caused by non-flat frequency responses of link components, a relative power comparison function (PCF) is widely used to construct RF frequency-to-power mapping. In the SD-DPMZM case, we can construct relationship between PCF and φ_3 as

$$PCF(\varphi_3) = \frac{P_{out}(\varphi_3|_{t_1})}{P_{out}(\varphi_3|_{t_1'} = \varphi_3|_{t_1} + \frac{\pi}{2})} \tag{2}$$

where $\varphi_3|_{t_1}$ and $\varphi_3|_{t_1'}$ are bias phases of twice dependent measurements at the time t_1 and t_1'. The bias phase difference between two dependent measurements is fixed at $\pi/2$ which is determined by MZM3 inherent half-wave voltage. The two-stage measurement can be performed after establishing relationship between PCF and φ_3.

2.1. *Coarse measurement*

The coarse estimation of the unknown RF frequency $\tilde{\Omega}$ can be calculated directly from the inverse function of Eq. (2) as

$$\tilde{\Omega} = f(\varphi_3|_{t_1}) = \sqrt{\frac{2(arccot(\sqrt{PCF(\varphi_3|_{t_1})}) - \varphi_3|_{t_1})}{\beta_2 \cdot L}} \tag{3}$$

Since φ_3 is only dependent on the bias of the MZM3, we can flexibly choose an arbitrary $\varphi_3|_{t_1}$ to calculate the coarse estimation.

2.2. *Fine measurement*

To achieve a potential high accuracy point implied by Eq. (3), we can subsequently choose the bias point $\varphi_3^*|_{t_2}$ by knowing $\tilde{\Omega}$

$$\varphi_3^*|_{t_2} = -\frac{\beta_2 \cdot L}{2}\tilde{\Omega}^2 \tag{4}$$

It is noticed that the derivative $\frac{\partial f(\varphi_3)}{\partial PCF}|_{\varphi_3^*} \doteq 0$, which means the measurement frequency is non-sensitive to PCF error at all. By shifting the bias point to $\varphi_3^*|_{t_2}$ in the second round measurement, the frequency with highest accuracy Ω^* can be achieved by calculating

$$\Omega^* = f(\varphi_3^*|_{t_2}) \tag{5}$$

#154886 - $15.00 USD Received 19 Sep 2011; revised 4 Nov 2011; accepted 14 Nov 2011; published 5 Dec 2011

3. Experimental setup

Figure 2 shows the system configuration to verify the proposed high accuracy frequency measurement methodology by systematically performing bias manipulations described above. A simulated unknown signal output from a RF synthesizer is modulated onto an optical carrier at 1549.8nm in a DPMZM. The modulator is characterized by performing pre-measurements to quantify the bias voltages for the single-drive configuration and to find the linear modulation region. Subsequently, the modulated optical signal is launched into a 35.5km single mode fiber (SMF) link and detected by a photodiode (PD). The optical power before the PD is fixed at 0dBm to avoid saturation effect. The power of the dispersion-induced fading signal is monitored by a RF powermeter. After analog to digital conversion, the digitalized power values are used to calculate PCFs and RF frequencies implemented in MATLAB. The system is running automatically by employing program-based GPIB instrument control interface in MATLAB as well where the RF reference frequencies and applied bias voltages are systematically programmed and controlled. In the digital domain, the frequency measurement procedure is divided into coarse and fine measurement stages as described above. The coarse frequency $\tilde{\Omega}$ is estimated based on Eq. (3) with the fixed bias phase $\varphi_3|_{t_1} = 0$. By using the coarse measured frequency $\tilde{\Omega}$, we can approximately calculate the bias point $\varphi_3^*|_{t_2}$ for highest accuracy using Eq. (4). The control module then switches the DC bias of the MZM3 to $\varphi_3^*|_{t_2}$ and refines the measurement process by calculate frequency using Eq. (5). In our experiment, the fine measurement stage is executed iteratively for ten times and the output values are averaged as the final frequency estimation.

For the proposed scheme, the frequency measurement range is determined by the first frequency notch point (fiber length) from Eq. (1). Taking 35.5km fiber for an example, the first power fading point is ∼10GHz, which indicates in a measurement range of 10GHz, each PCF value is corresponding to only one frequency. On the contrary, if considering a measurement range beyond 10GHz, a PCF value will be corresponding to multiple frequency point, which will induce measurement ambiguity during frequency estimation. On the other hand, the fiber length also affects the measurement accuracy. To clarify this, we assume the fiber length $L_2 > L_1$. When $\varphi_3 \doteq \varphi_3^*$, from Eq. (3), we can get $\frac{\partial f}{\partial PCF}|_{L_2} < \frac{\partial f}{\partial PCF}|_{L_1}$. So for a fixed PCF deviation, the accuracy with a longer fiber is better than that with a shorter fiber. Therefore, the measurement range and the accuracy is a trade off and can be balanced by adjusting the fiber length.

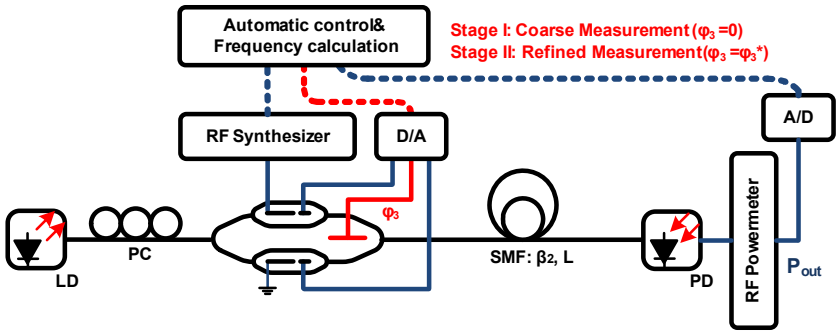

Fig. 2. Experimental setup of the high accuracy frequency measurement system. LD: laser diode. PC: polarization controller. PD: photodiode. A/D and D/A: analog to digital converter and digital to analog converter.

#154886 - $15.00 USD Received 19 Sep 2011; revised 4 Nov 2011; accepted 14 Nov 2011; published 5 Dec 2011

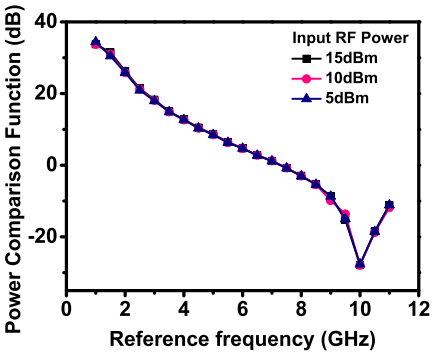

Fig. 3. Coarse measurement stage: PCF versus input RF frequency for different RF power.

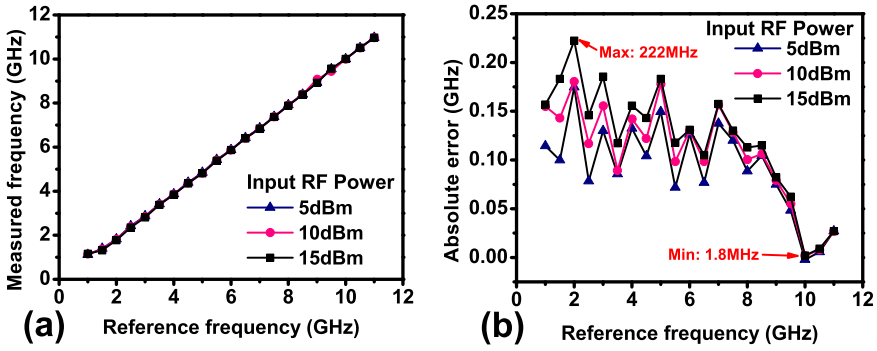

Fig. 4. Coarse measurement stage: **(a)** Measured RF frequency versus input reference frequency for different RF power. **(b)** Absolute measurement error versus input reference frequency for different RF power.

4. Experimental results

The coarse measurement procedure is executed for different RF input powers of 5dBm, 10dBm and 15dBm. The PCF value with respect to the reference frequencies for different RF input powers is shown in Fig. 3. The first power fading notch is at ∼10GHz. For the reference RF frequency beyond the notch point, the PCF value will be the same with another corresponding frequency, which implies the unambiguous frequency measurement range is confined by the first notch point. To adjust the measurement range, it is applicable to change the dispersion amount of the optical link. Figure 4(a) shows the measured frequencies obtained from Eq. (3) as a function of reference frequencies for different input power levels. It can be seen that the estimated values agree linearly with the reference values and the measurements are consistent for different input powers. The errors between the measurement and the reference are shown in Fig. 4(b). The error curves fluctuate in a range from a minimum of 1.8MHz to a maximum of 222MHz with the average error of 118MHz. The error curve drops significantly when the reference frequency is close to 10GHz because for a 35.5km SMF, the highest accuracy requirement of the bias point is $\varphi_3^*|_{t_2} \doteq 0$, which is almost satisfied in the coarse measurement case. Figure 5 shows the fine measurement results for 10dBm RF input by setting the bias point $\varphi_3 = \varphi_3^*|_{t_2}$. Figure 5(a) shows the error limits of the ten times iterative fine measurements. The absolute error fluctuation is less than 5MHz with the average error of 5.4MHz, which shows the stability of the fine measurement process. The absolute error comparison between the coarse and fine measurements is shown in Fig. 5(b). By performing a high accuracy measurement, the average uncertainty of the measured frequency can be tremendously decreased from 118MHz to 5.4MHz, which implies that a relative error of $\sim 10^{-3}$ is achieve by using the proposed method.

#154886 - $15.00 USD Received 19 Sep 2011; revised 4 Nov 2011; accepted 14 Nov 2011; published 5 Dec 2011

In the experiment, bias drift of the modulator is the main negative factor affecting the accuracy and the stability of the measurement. Figure 6 shows the fine measurement error with the MZM3 bias voltage drift for 10GHz reference frequency considering the non-ideal biasing characteristics of the DPMZM. In this case, the bias drift is emulated by intentionally inducing a deviation from φ_3^*. A ∼60MHz/V degradation of measurement performance is observed.

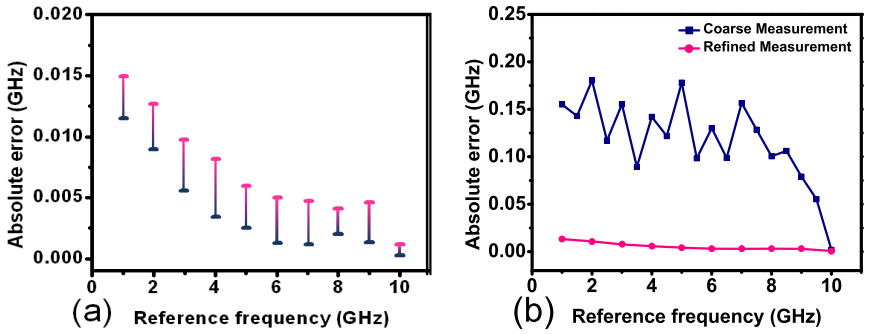

Fig. 5. Fine measurement stage: **(a)** Error range for ten times fine measurements. **(b)** Error comparison of coarse and fine measurement.

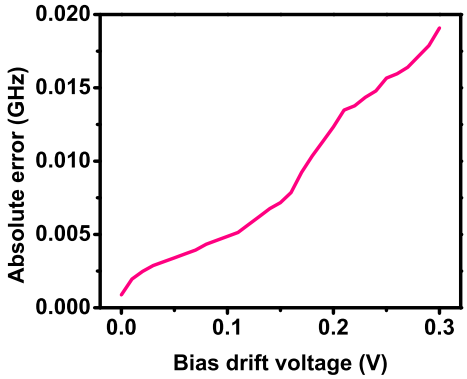

Fig. 6. Absolute error effected by the MZM3 bias drift.

5. Conclusions

A novel scheme for high accuracy broadband microwave frequency measurement is proposed. Based on a SD-DPMZM, the highest accuracy bias point is theoretically derived and the methodology to achieve highest accuracy measurement is systematically presented. Based on frequency-to-power mapping technique, our proposed two-stage microwave frequency measurement system is experimentally demonstrated. The system performs well with a decreased relative error of 10^{-3} within a 10GHz measurement range. The proposed approach shows an unprecedented improvement of measurement uncertainty and proves the increased applicability for future electronic warfare applications with high accuracy demands.

Acknowledgments

This work was supported in part by National Nature Science Foundation of China (NSFC) under grant No. 60736003, 61025004, 61032005, National 863 Program under grant No. 2009AA01Z222, 2009AA01Z223 and National Basic Research Program of China under grant No 2012CB315603-04.

#154886 - $15.00 USD Received 19 Sep 2011; revised 4 Nov 2011; accepted 14 Nov 2011; published 5 Dec 2011